Impact of bioenergy crops expansion on climate-carbon cycle feedbacks in overshoot scenarios

Irina Melnikova[1,2], Olivier Boucher[1], Patricia Cadule[1], Katsumasa Tanaka[2,3], Thomas Gasser[4], Tomohiro Hajima[5], Yann Quilcaille[6], Hideo Shiogama[3], Roland Séférian[7], Kaoru Tachiiri[3,5], Nicolas Vuichard[2], Tokuta Yokohata[3] and Philippe Ciais[2]

[1]Institut Pierre-Simon Laplace (IPSL), Sorbonne Université / CNRS, Paris, France
[2]Laboratoire des Sciences du Climat et de l'Environnement (LSCE), IPSL, Commissariat à l'énergie atomique et aux énergies alternatives (CEA/ CNRS/ UVSQ), Université Paris-Saclay, Gif-sur-Yvette, France
[3]Earth System Division, National Institute for Environmental Studies (NIES), Tsukuba, Japan
[4]International Institute for Applied Systems Analysis (IIASA), Laxenburg, Austria
[5]Research Institute for Global Change, Japan Agency for Marine-Earth Science and Technology, Kanazawa-ku, Japan
[6]Institute for Atmospheric and Climate Science, ETH Zürich, Switzerland
[7]CNRM, Université de Toulouse, Météo-France, CNRS, Toulouse, France

Correspondence to: Irina Melnikova (irina.melnikova@lsce.ipsl.fr)

Abstract. Stringent mitigation pathways frame the deployment of second-generation bioenergy crops combined with Carbon Capture and Storage (CCS) to generate negative CO_2 emissions. This Bioenergy with CCS (BECCS) technology facilitates the achievement of the long-term temperature goal of the Paris Agreement. Here, we use five state-of-the-art Earth System models (ESMs) to explore the consequences of large-scale BECCS deployment on the climate-carbon cycle feedbacks under the CMIP6 SSP5-3.4-OS overshoot scenario keeping in mind that all these models use generic crop vegetation to simulate BECCS. First, we evaluate the land cover representation by ESMs and highlight the inconsistencies that emerge during translation of the data from integrated assessment models (IAMs) that are used to develop the scenario. Second, we evaluate the land-use change (LUC) emissions of ESMs against bookkeeping models. Finally, we show that an extensive cropland expansion for BECCS causes ecosystem carbon loss that drives the acceleration of carbon turnover and affects the CO_2 fertilization effect- and climate change-driven land carbon uptake. Over the 2000–2100 period, the LUC for BECCS leads to an offset of the CO_2 fertilization effect-driven carbon uptake by 12.2% and amplifies the climate change-driven carbon loss by 14.6%. A human choice on land area allocation for energy crops should take into account not only the potential amount of the bioenergy yield but also the LUC emissions, and the associated loss of future potential change in the carbon uptake. The dependency of the land carbon uptake on LUC is strong in the SSP5-3.4-OS scenario but it also affects other SSP scenarios and should be taken into account by the IAM teams. Future studies should further investigate the trade-offs between the carbon gains from the bioenergy yield and losses from the reduced CO_2 fertilization effect-driven carbon uptake where BECCS is applied.

1 Introduction

All stringent future socio-economic mitigation scenarios have negative emissions that rely on carbon dioxide removal (CDR) technologies (Fuss et al., 2014, Rogelj et al., 218). CDR is important especially in overshoot scenarios, in which temperature temporarily exceeds the given target, e.g., the Paris Agreement temperature target, before ramping down as CO_2 is withdrawn artificially from the atmosphere (Jones et al., 2016a; Keller et al., 2018; Tanaka et al., 2021).

40   Bioenergy with Carbon Capture and Storage (BECCS) is one of the most cost-effective CDR technologies (Jones
41   and Albanito, 2020; Babin et al., 2021). In BECCS, atmospheric CO_2 is captured from biomass growth, and the
42   harvested biomass is then converted into bioenergy or directly combusted and a fraction of the carbon contained
43   in the CO_2 produced is recuperated and is stored in geological reservoirs without being released back to the
44   atmosphere (Canadell and Schulze, 2014). BECCS is a nascent CDR technology that has not been proven at large
45   spatial scales. Its potential advantages include technical feasibility and a relatively low discounted cost in future
46   decades that allows spreading mitigation efforts over a longer period (Anderson and Peters, 2016; Dooley et al.,
47   2018).

48   The limitations of BECCS are the requirement of potentially large land areas, a loss of biodiversity, and the need
49   for extra water and nutrients (Heck et al., 2018; Séférian et al., 2018; Li et al., 2021). Besides, BECCS may lead
50   to a large amount of carbon emissions from land-use change (LUC), when bioenergy crops are grown over high-
51   carbon content ecosystems such as grassland and forest (Clair et al., 2008; Gibbs et al., 2008; Schueler et al.,
52   2013; Smith et al., 2016; Harper et al., 2018; Whitaker et al., 2018). The LUC emissions released due to land
53   conversion to bioenergy crops include immediate (direct) greenhouse gas (GHG) emissions associated with the
54   destruction of biomass and slash during LUC but also delayed (indirect) emissions from the decay of stumps and
55   soil carbon. These emissions are termed as "carbon debt" (Clair et al., 2008; Fargione et al., 2008; Gibbs et al.,
56   2008; Krause et al., 2018) because for BECCS to be carbon neutral, this loss of carbon must be paid back by
57   several cycles of BECCS harvest followed by carbon geological storage, assumed to substitute with fossil carbon
58   emissions. Using low-productivity marginal or degraded lands for the deployment of second-generation bioenergy
59   crops (such as miscanthus or switchgrass) reduces the carbon debt because such lands have less carbon to lose.
60   Further, soil carbon sequestration, in the long run, may even be achieved with BECCS if non-harvested residues
61   of BECCS crops exceed the carbon input to the soil of the native ecosystems they substitute (Campbell et al.,
62   2008; Gibbs et al., 2008; Mohr and Raman, 2013; Whitaker et al., 2018).

63   The issue with putting second-generation bioenergy crops in low-productivity lands is a need to invest large areas
64   of land (Jones et al., 2016a; Smith et al., 2016). Currently, some land ecosystems act as a carbon sink primarily
65   driven by the CO_2 fertilization effect on photosynthesis and the carbon turnover in ecosystems. As croplands,
66   unlike other ecosystems, have limited potential to store additional carbon because the biomass is harvested
67   regularly, and as the new croplands have a lower soil carbon stock with a short turnover time for soil carbon, the
68   large-scale BECCS deployment must affect the land carbon uptake, although this has not been specifically looked
69   at in Earth System Models (ESMs) simulation results. No study to date has estimated the effects of BECCS
70   deployment on the terrestrial carbon cycle under an overshoot scenario.

71   In this study, we estimate the impact of large-scale BECCS deployment on the carbon-climate feedbacks under
72   the Shared Socioeconomic Pathway (SSP) overshoot scenario named SSP5-3.4-OS that includes mitigation
73   policies via an increase in the land area covered by second-generation bioenergy crops for CDR (Hurtt et al.,
74   2020). We use simulations from five Coupled Model Intercomparison Project 6 (CMIP6) ESMs to estimate LUC
75   impacts on the changes in land carbon uptake and carbon-climate feedbacks.

2 Data and methods

2.1 SSP5-3.4-OS scenario

The SSP5-3.4-OS follows the high-emission SSP5-8.5 scenario and branches from it in 2040 when aggressive mitigation policies are implemented (O'Neill et al., 2016; Meinshausen et al., 2020). The delayed mitigation leads to an overshoot of the Paris Agreement 2 °C temperature limit. In addition to a decline in fossil fuel emissions, mitigation efforts after 2040 include the expansion of second-generation bioenergy crops (for BECCS) at the cost mainly of pasture lands (Hurtt et al., 2020). There is no deforestation assumed after 2010, in order to preserve the areas with high carbon content. Second-generation bioenergy crops account for most of the new cropland areas deployed after 2040.

2.2 CMIP6 ESMs

We use five CMIP6 ESMs that simulate the SSP5-3.4-OS (Table 1). In addition to fully coupled simulations (COU), biogeochemically (BGC) coupled simulations, where only changes in the atmospheric CO_2 concentration, and not the temperature, affect the carbon-cycle processes, are also provided as part of the Coupled Climate–Carbon Cycle Model Intercomparison Project (C4MIP) (Jones et al., 2016b). The combination of COU and BGC simulations allows us to study carbon-climate feedbacks. The BGC simulation outputs indicate the changes in the carbon fluxes driven by the CO_2 fertilization effect, the difference between COU and BGC simulations indicates the changes in the carbon fluxes driven by climate change.

The LUC emissions in the ESMs can be estimated as the difference in net biome production (NBP) between simulations with and without land-use change that is between the "historical" and "hist-noLu" simulations for the historical period. However, simulation pairs for future scenarios such as SSP5-3.4-OS are not usually available. The "fLuc" (net carbon mass flux into the atmosphere due to LUC) variable provided by some ESMs enables an alternative way to incompletely quantify direct LUC emissions that include deforestation (biomass loss during deforestation), wood harvest, and the release of CO_2 by harvested wood products, but exclude forest regrowth and legacy soil carbon decay or gains. Three models, IPSL-CM6A-LR, CNRM-ESM2-1, and UKESM1-0-LL under consideration, provide the variable "fLuc" (Table 1).

Gridded CMIP6 data, with the exception of the "fLuc" variable, were adjusted by subtracting the long-term pre-industrial linear trend from the control (piControl) experiment at a grid level. We used the anomalies relative to the branching year values (indicated in Table S1) for changes in carbon pools and long-term mean piControl values for changes in carbon fluxes.

2.3 Methodology

ESMs do not provide necessary outputs to diagnose the specific carbon fluxes generated from the transitions to bioenergy crops: 1) they do not treat energy crops explicitly but rather use a generic "crop" vegetation type, itself being a grass with a higher photosynthesis rate in some models, 2) crops only cover a fraction (tile) of a model grid box, and 3) the soil carbon pool is usually not split into tiles for each vegetation type in land surface models. Hence there is no perfect way to diagnose such fluxes. We pragmatically decompose the global changes in land carbon uptake to the contributions that are LUC- and noLUC-induced by using three different approaches described below.

113   In the *"fLuc" approach (1)*, we exploit the "*fLuc*" variable provided by most models in CMIP6.

114   The global carbon flux, NBP that includes changes in ecosystems both with LUC and noLUC effects, cumulated

115   over time, approximates the changes in the land carbon pool. Thus, cumulative NBP + fLuc (because NBP and

116   fLuc have opposite sign conventions with NBP positive sink to land) approximates the changes in the land carbon

117   pool of noLUC ecosystems.

118   *In the "cropland threshold" approach (2)*, we divide the global land area into energy-crop-concentrated and no-

119   energy-crop (not energy-crop-concentrated) grid cells by taking into account their evolution after 2015. Hurtt et

120   al. (2020) reported that after 2040, cropland areas expanded "mainly due to large-scale deployment of second-

121   generation bioenergy crops". We carry out a sensitivity study (Text A1) to label the given grid cell as crop-

122   concentrated if the cropland fraction of the grid cell is larger than a given threshold. In the sensitivity analysis, we

123   examine a range of post-2015 cropland fraction thresholds of the grid box area and select the (ESM-specific)

124   thresholds that best approximate the total cropland area change in 2015–2100 diagnosed by each ESM.

125   Under this approach, the treatment of LUC and noLUC lands and the attribution of the LUC effects on the carbon

126   uptake that are relevant to BECCS are both spatially explicit. The disadvantage of this approach is that by sampling

127   an arbitrary fraction of crop-concentrated grid-cells, we inevitably omit some carbon changes in cropland or

128   encroach carbon belonging to non-crop vegetation.

129   *In the "two simulations" approach (3),* we performed additional SSP5-3.4-OS scenario simulations by IPSL-

130   CM6A-LR and MIROC-ES2L. In addition to standard SSP5-3.4-OS and SSP5-3.4-OS-BGC simulations, we

131   performed simulations in which land use is held constant corresponding to the 1850 usage (SSP5-3.4-OS-

132   noLUC1850 and SSP5-3.4-OS-noLUC1850-BGC). In addition, using IPSL-CM6A-LR, we performed

133   simulations with 2040 land cover usage (SSP5-3.4-OS-noLUC2040 and SSP5-3.4-OS-noLUC2040-BGC). The

134   difference in NBP between simulations with and without LUC indicates LUC emissions, which are dominated by

135   bioenergy crops area expansion after 2040. Unlike in approaches (1) and (2), the term LUC here incorporates a

136   carbon source called the "loss of additional sink capacity" (LASC) relative to the reference years 1850 and 2040

137   (Gasser and Ciais, 2013; Pongratz et al., 2014). LASC is a change in carbon flux, or a foregone sink, in response

138   to environmental changes on managed land compared to potential natural vegetation. The approach (3) accounts

139   for the indirect LUC emissions while the approaches (1) and (2) do not.

140   **3 Evaluation and data consistency**

141   The SSP5-3.4-OS is a concentration-driven scenario based on the implementation of SSP5 in the REMIND-

142   MAgPIE integrated assessment model (IAM) (Kriegler et al., 2017; Meinshausen et al., 2020). Bauer et al. (2017),

143   Popp et al. (2017), and Riahi et al. (2017) provided additional details on the changes in energy and land use. Hurtt

144   et al. (2020) provided the changes in land use in a coherent gridded format required for ESMs in the Harmonization

145   of Global Land-Use Change and Management version 2 (LUH2) project. In LUH2, the historical data (up to the

146   year 2014) based on the History of the Global Environment database (HYDE) and future scenarios (2015–2300)

147   based on IAM are harmonized to minimize the differences between the end of historical reconstruction and IAM

148   initial conditions (Hurtt et al., 2020). The harmonization process, however, is expected to result in some

149   mismatches between LUH2 and the IAM during the early stage of the post-2014 period. First, we check the

150   consistency of the global and regional cropland and other land-state areas reported by REMIND-MAgPIE, LUH2,

151 and CMIP6 ESMs. Second, we evaluate global and regional historical LUC estimates by CMIP6 ESMs against

152 three bookkeeping approaches.

3.1 Consistency of cropland area between REMIND-MAgPIE, LUH2, and ESMs

154 Under the SSP5-3.4-OS pathway, the cropland area increases by 8.1×10^6 km^2 (~50%) from the 2010 level in the

155 21st century to 2100 (Hurtt et al., 2020). The global cropland area modelled by REMIND-MAgPIE and

156 downscaled by LUH2 increases due to the expansion of second-generation bioenergy crops. The global cropland

157 areas by REMIND-MAgPIE and LUH2 are largely consistent with a slightly larger area of crops by REMIND-

158 MAgPIE till the 2050s (reaching 0.6×10^6 km^2 in the year 2050) and a larger area of crops by LUH2 in 2060 –

159 2090s (Figure 1a). Unlike the REMIND-MAgPIE, LUH2 simulates a slight reduction of forest area (by 1.3×10^6

160 km^2 in 2100 from 2010 level). The global cropland area in LUH2 is less than in REMIND-MAgPIE by 0.3×10^6

161 km^2 in 2015, and larger by 2.9×10^6 km^2 in 2060 that is 14% of the total cropland area of 20.7×10^6 km^2 by LUH2

162 in 2060 (and corresponds to a 43.4% increase from the 2015 level) and may cause additional uncertainty in

163 estimates of the BECCS area and LUC. Further, ESMs implement the global and regional gridded cropland

164 fractions following LUH2 and using their own land cover map (Figure 1b), with an exception of UKESM1-0-LL

165 that reports an evolution of the global cropland area smaller than those of other ESMs. This deviation of UKESM1-

166 0-LL may occur because of its specifications in the treatment of croplands and the model's dry bias (precipitation

167 deficit) in India and the Sahel (Sellar et al., 2019). While the model uses the LUH2 data to prescribe an area

168 available for crops to grow in, this area is covered by the crop PFTs only if the model's climate is suitable for the

169 grass PFTs, otherwise, the area remains bare soil.

170 Aside from the deviations in total areas of land cover types between REMIND-MAgPIE, LUH2, and ESMs listed

171 above, a discrepancy arises from the implementation of LUH2's land cover types to the ESM's plant functional

172 types (PFTs). Nevertheless, most CMIP6 ESMs produce croplands area consistent with LUH2. However, the other

173 vegetation classes of LUH2 (e.g., forested lands, non-forested lands, pastures) do not match the PFTs of ESMs

174 because most ESMs decided to use their own land cover map rather than used the LUH2 one for these ecosystems.

175 First, spatial distributions of vegetation classes are tightly associated with climate and biogeochemical processes,

176 and thus, the replacement of the vegetation covers in ESMs would lead to large changes in the model

177 performances. Second, some models that include dynamic vegetation, like UKESM1-0-LL, predict the vegetation

178 distribution change, and sometimes the predicted distribution does not coincide with the one prescribed by LUH2.

179 Besides, the pastures of REMIND-MAgPIE are translated to two land-use states in LUH2: pastures and

180 rangelands. While they are treated predominantly as low-productivity areas in REMIND-MAgPIE, this may not

181 be a case in ESMs, where pastures and rangelands may correspond to grasslands and perhaps to shrublands (if

182 this land cover exists in an ESM). Some ESMs do not distinguish pastures and rangelands because of the ambiguity

183 in their definitions. Likewise, the SSP5-3.4-OS scenario involves large-scale second-generation bioenergy crops

184 whose benefit is the capability to grow in so-called "marginal" lands (Krause et al., 2018). The ambiguity and

185 inconsistency in the definition of land-use and land-cover tiles between IAM, LUH2, and ESMs may have

186 implications for the interpretation of the scenario.

187 We shed light on an issue of inconsistency when translating LUC from IAMs into LUH2 and, then, into ESMs.

188 Overall, implementation of the LUC scenario of REMIND-MAgPIE to first, LUH2, and then ESMs leads to a

189 consistency loss of simulated scenario during the harmonization process. Further, the land cover representation in

190   ESMs is subjective and different from the IAM and LUH2 mainly because of ambiguity in the correspondence

191   between land-use and vegetation type definitions. This problem requires thorough attention, especially in ESMs

192   and IAMs intercomparison studies.

193   **3.2 Evaluation of land-use change emissions**

194   The global and regional LUC emissions estimated by ESMs were evaluated against three bookkeeping models for

195   the historical period, namely BLUE (Hansis et al., 2015), HN2017 (Houghton and Nassikas, 2017), and OSCAR

196   (Gasser et al., 2020). The models differ in the spatial units (spatially explicit, country level, region level),

197   parametrization, and process representations (Friedlingstein et al., 2020; Gasser et al., 2020). Unlike other

198   bookkeeping models, OSCAR also reported LASC in LUC estimates but the utilized version did not include peat

199   emissions.

200   Unlike the difference in NBP between simulations with and without LUC, the "fLuc" variable accounts only for

201   the direct LUC emissions and does not account for all the fluxes reported by bookkeeping models, e.g., forest

202   regrowth and slash and soil organic matter decay, as well as for shifting cultivation and degradation (Houghton

203   and Nassikas, 2017). Thus, its values are expected to be lower. We use an average of multiple realizations when

204   provided by the model teams (details in Table S1). The evaluation targets estimating LUC emissions in "fLuc"

205   and "two simulations" approaches.

206   We found that ESMs tend to estimate lower global LUC emissions than bookkeeping models by both "fLuc"

207   variable and "two simulations" approaches (Figure 2). This is remarkable in the three tropical regions that

208   dominate global LUC emissions since the 1960s, and particularly South and Southeast Asia (Figure S1). In 1960–

209   2014, on average, bookkeeping models estimate that three tropical regions account for $56.8 \pm 2.3\%$ of global LUC

210   emissions, while ESMs estimate that they account for $35 \pm 10\%$ based on simulations with and without LUC and

211   $40 \pm 15\%$ based on the "fLUC" variable.

212   LUC emission estimates by MIROC-ES2L (for which only LUC emissions derived from simulations with and

213   without LUC were available) are the most consistent with the estimates of bookkeeping models among considered

214   ESMs (see also Liddicoat et al., 2021). We excluded the estimates of LUC emissions by CNRM-ESM2-1 based

215   on simulations with and without LUC and by UKESM1-0-LL based on "fLuc" from the analysis. CNRM-ESM2-

216   1 estimates much lower LUC emissions derived from simulations with and without LUC than other ESMs,

217   possibly because the CMIP6 version of the model does not include a harvest module, i.e., croplands are modelled

218   as natural grasslands (Séférian et al., 2019), and cropland soils continue to be loaded by harvest inputs. UKESM1-

219   0-LL estimates implausibly low LUC emissions derived from the "fLuc" variable.

220   The LUC emissions estimated by the two approaches differ remarkably due to inconsistent "fLuc" definitions

221   among models (Gasser and Ciais, 2013). We call for a clearer and more rigorous definition of this variable in

222   future MIPs so that model outputs can be compared on the same basis. As some examples for improvement, we

223   suggest that model teams provide explicit detail of processes that contribute to "fLuc", e.g., direct deforestation

224   and wood harvest emissions, decomposition flux, as well as indirect emissions, e.g., per each PFT.

225   **3.3 Evaluation of land-use change emissions from BECCS deployment**

226   The increased LUC emissions to account for BECCS are a part of total carbon budget calculations in the IAM

227   scenario. We compared LUC emissions by different approaches using ESMs with LUC of REMIND-MAgPIE

228   (Figure S2). While the IAMs design the scenario in a way that the benefits of BECCS exceed the carbon losses

229   from LUC, the ability of IAM to accurately estimate LUC emissions including legacy emissions is questionable.

230   In the SSP5-3.4-OS scenario, the REMIND-MAgPIE estimates lower LUC emission compared ESMs.

231   BECCS dominates negative emissions in the SSP5-3.4-OS pathway. We confirmed that BECCS is predominantly

232   deployed in low-carbon uptake areas by comparing the changes in carbon pools and NBP globally and crop-

233   concentrated areas (Figure S3). Because bioenergy crops are deployed in low-carbon uptake areas and they

234   dominate LUC emissions in the 21st century, the NBP over crop-concentrated areas derived by the "cropland

235   threshold" approach approximates global LUC emissions. The comparison of NBP in crop-concentrated grids

236   with the original LUC emissions of the REMIND-MAgPIE IAM scenario confirms a similar trend between IAM-

237   based global LUC emissions and ESMs-based global temporal NBP changes in the crop-concentrated areas after

238   2040. The strong correlation is evident in three ESMs, namely CanESM5, UKESM1-0-LL, and MIROC-ES2L

239   (correlation coefficient is 0.72 for the 2015–2100 period). The carbon loss in the crop-concentrated areas over the

240   21st century period averaged over these three ESMs reaches 37.8 ± 30.3 GtC. Two models, IPSL-CM6A-LR and

241   CNRM-ESM2-1, however, do not capture the increased carbon loss after 2040 perhaps due to low estimates of

242   LUC emissions from crop expansion (especially CNRM-ESM2-1) or overestimated uptake by no-LUC areas

243   (Figures 2, S1). Besides, IPSL-CM6A-LR simulates the lowest ecosystem carbon pool, especially in soils (Arora

244   et al., 2020) that may lead to relatively small LUC-induced carbon losses when cropland areas expand. Thus, the

245   estimates of LUC impact on carbon-climate feedbacks from IPSL-CM6A-LR and CNRM-ESM2-1 need to be

246   considered with the above-mentioned caveats.

247   **4 The impact of LUC from bioenergy crops expansion on the carbon uptake**

248   **4.1 Differences in LUC impact on carbon uptake estimated by three approaches**

249   We use the estimates of the LUC impacts on global carbon uptake by IPSL-CM6A-LR and MIROC-ES2L to

250   compare the three approaches described in section 2.3. The estimates of both models and three approaches show

251   that the LUC impacts lead to a loss of carbon fluxes (Figure 3). The losses from LUC surpass the benefits from

252   the CO_2 fertilization effect, so that the LUC ecosystems become a carbon source to the atmosphere. The "cropland

253   threshold", unlike the other two approaches, separates cropland-concentrated and no-crop contributions spatially.

254   Thus, the estimated changes in carbon uptake are areal cumulative under the "cropland threshold" approach. In

255   the other two approaches, in contrast, the changes in carbon fluxes are calculated in each grid cell for both LUC-

256   dominated and noLUC ecosystems, so that carbon change of these two land-use categories may partly offset each

257   other.

258   A larger loss is seen in "two simulations since 1850" because these simulations include LASC and legacy soil

259   emissions (Figure 3a). Intermediate loss is from "fLUC" because this approach includes only immediate (direct)

260   carbon loss. Lower carbon losses correspond to the "cropland threshold" approach that also includes a carbon sink

261   in natural ecosystems over selected grid cells and misses initial carbon loss, and to "two simulations since 2040"

262   that misses legacy emissions of activities before 2040. The larger carbon losses in the "two simulations since

263   1850" than in the "two simulations since 2040" estimates also reveal the long-term effects of LUC.

264   In the case of IPSL-CM6A-LR, the "cropland threshold" and "two simulations since 2040" approaches produce

265   similar estimates of LUC impact on cumulative land carbon uptake because these two methods target the changes

266 in the carbon fluxes, particularly due to cropland expansion for BECCS in the 21st century. MIROC-ES2L that

267 accounts for gross LUC emissions (Liddicoat et al., 2021) produces similar estimates of LUC impact by "cropland

268 threshold" and "two simulations since 1850" approaches.

4.2 Temporal impacts of LUC on global carbon uptake

270 Figure 4 illustrates the attribution of global carbon fluxes to LUC- (or crop-concentrated) and no-LUC (no-crop)

271 ecosystems by five ESMs and three approaches (see Figure S4 for the results, specific for each ESM and

272 approach). The large-scale deployment of bioenergy crops even on low carbon-uptake areas causes a carbon loss

273 from the ecosystem. The negative values of the carbon flux in the CO_2 concentration only simulation indicate the

274 domination of the LUC losses over the CO_2 fertilization effect-driven carbon gains in the ecosystems.

275 For the "cropland threshold" approach, the majority of ESM simulations, excluding IPSL-CM6A-LR and CNRM-

276 ESM2-1 (see section 3.3), agree that cropland expansion causes a decrease in global CO_2 fertilization effect-driven

277 carbon uptake, especially in crop-concentrated grids which lose carbon from LUC. Cropland expansion for

278 BECCS may also contribute to the global climate change-driven carbon loss. However, these changes are small

279 in the "cropland threshold" and absent in "fLUC" estimates. We speculate this occurs because the "fLuc" variable

280 involves only direct LUC changes such as deforestation, wood harvest, and soil carbon decay. On top of it, earlier

281 findings show that the ESMs do not realistically represent the dynamics of soil and litter carbon after LUC (Boysen

282 et al., 2021). The LUC carbon losses for BECCS deployment cannot be overridden by the increased CO_2 effects

283 but they contribute to the carbon losses driven by climate change. Overall, the three approaches and five ESMs

284 demonstrate that the BECCS expansion under the SSP5-3.4-OS pathway results in 42.55 ± 41.08 GtC loss that

285 corresponds to 12.2% of noLUC CO_2 fertilization-driven uptake and to an additional 13.00 ± 12.27 GtC loss that

286 corresponds to 14.6% of noLUC climate change-driven loss over the 2000–2100 period (Table S2).

4.3 Spatial variation of impacts of LUC on global carbon uptake

288 We investigated the spatial variation of LUC impact on the land carbon cycle using simulations with and without

289 LUC by MIROC-ES2L and IPSL-CM6A-LR (Figure 5). Two models show that the carbon uptake decreases in

290 the BECCS areas due to LUC emissions. Even though the SSP5-3.4-OS scenario is designed so that BECCS

291 utilizes low carbon areas to cause the least possible impact on the carbon sink in unmanaged lands, these BECCS

292 areas lose their CO_2 fertilization-driven carbon uptake potential but do not escape climate change-driven carbon

293 losses. In the SSP5-3.4-OS scenario, second-generation biofuel cropland areas estimated by LUH2 reach nearly

294 6% of global land (potentially vegetated) area in 2100. Assigning such vast areas to bioenergy crops – even if

295 they correspond to low-carbon content ecosystems – affects the land carbon uptake and the global carbon cycle

296 feedbacks. The decision on the assignment of these areas for energy crops requires assessment of both the current

297 state of the ecosystem, e.g., the carbon content in vegetation and soil, and the future potential increase in the

298 carbon uptake. The impact of LUC on the carbon cycle should be accounted for in developing future mitigation

299 pathways so that the benefits of BECCS are not minimized by the carbon losses.

5 The carbon cycle feedback framework perspective

The CO_2 fertilization effect- and climate change-driven changes in the carbon fluxes and storages may be expressed as β and γ feedback parameters per unit changes in the global atmospheric CO_2 concentration (ΔCO_2) and surface air temperature (ΔT), respectively (Jones et al., 2016b; Friedlingstein et al., 2020; Zhang et al., 2021). Here the temperature change is taken as a proxy for the response of the ecosystem carbon storage to climate change. The carbon-concentration β (GtC ppm^{-1}) and carbon-climate γ (GtC °C^{-1}) feedback parameters can be estimated using BGC and COU simulation outputs (Friedlingstein et al., 2006; Gregory et al., 2009; Jones et al., 2016; Melnikova et al., 2021; Zhang et al., 2021):

$$\beta = \frac{\Delta C_{BGC}}{\Delta CO_2}, \tag{1}$$

$$\gamma = \frac{\Delta C_{COU} - \Delta C_{BGC}}{\Delta T} , \tag{2}$$

where ΔC_{BGC} and ΔC_{COU} indicate the changes in the land carbon pool (or cumulative uptake) in BGC and COU simulations, respectively, and ΔCO_2 and ΔT (from COU runs) indicate the changes in the global CO_2 concentration and mean surface air temperature, respectively, all reported changes being relative to pre-industrial level (piControl).

The carbon cycle feedback framework is often compared between ESMs in idealized scenarios (such as 1%CO_2 increase), and the β and γ feedback parameters / metrics are assumed to be a pure response to the CO_2 concentration and temperature changes. Applying this framework to non-idealized and more socially relevant scenarios provides another perspective for understanding the changes in the carbon fluxes under more realistic evolutions. Previously, Melnikova et al. (2021) applied the β and γ framework to the SSP5-3.4-OS scenario and showed an amplification of the feedback parameters after the CO_2 concentration and temperature peaks due to inertia of the Earth system. Here we performed an estimation of the β and γ feedback parameters to investigate the impacts of the LUC on the behavior of the feedback parameters.

Note, in the case of the overshoot scenarios, if the CO_2 concentration and temperature changes during the ramp-down period went to zero, the definitions described in equations 1 and 2 would become invalid. Although because in this study, the change in CO_2 concentration and the temperature never goes to zero (in the SSP5-3.4-OS before 2300), and the feedbacks parameters can safely be calculated, the limitation should be taken into account.

The land carbon uptake and the β and γ feedback parameters are affected by LUC, so that they are lower in the simulations with LUC (Figure 6). Moreover, the difference in the β parameter estimated by IPSL-CM6A-LR in simulations with LUC and without LUC after the year 2040 suggests that even only LUC for bioenergy crops expansion affects the hysteresis behaviour of the carbon cycle feedback parameters under declining CO_2 concentration and temperature.

To date, the LUC impacts on the carbon cycle have not been included into the β and γ feedback framework, and the LUC emissions are discussed as an anthropogenic forcing separately from the feedbacks of land ecosystems to the changed CO_2 and climate. However, the β and γ parameters cannot be decoupled either from the state of the land use, or from the pre-industrial state of land cover, or from other model structural parts, leading to a value for equilibrium carbon stock. There is an interplay between land cover and the model's response to CO_2 (and climate) that has been demonstrated mathematically in Gasser & Ciais (2013) and defined as LASC. Gasser et al. (2020) quantified it as a foregone sink of about 30 GtC over the historical period. But this value can only increase as future CO_2 will be much higher than in the past.

In a broader sense, the land-cover and land-use associated differences in the initial conditions of ESMs simulations influence the estimates of global carbon cycle feedback parameters even under idealized pathways. The divergences in the pre-industrial land covers among ESMs lead to spatial differences in the ecosystem carbon stocks (e.g., ESM with larger forest cover has larger land carbon pool size). Furthermore, the pre-industrial levels of ecosystem carbon stock vary among models even for identical land-cover types. The estimated global β and γ feedback parameters involve these land-cover-related uncertainties. Future studies should address the issue by benchmarking the sets of idealized experiments with different types of land-cover and land-use changes.

6 Conclusion

In this study, we investigated the impacts of bioenergy crop deployment on the carbon cycle under an overshoot pathway. In the evaluation part of this study, we highlighted some inconsistencies in the land-use states and their temporal transitions between the REMIND-MAgPIE, LUH2, and ESMs. These differences arise from differences in process representations and initial conditions, as well as land-use and land-cover tiles definitions across models. The inconsistencies should be taken into account in comparative studies of IAMs and ESMs. Further work will be required to address the issue of the level of inconsistency between the IAMs, LUH2, and ESMs that should be tolerated to have confidence that ESMs and IAMs describe the same scenario.

We exploit five ESMs and three approaches to show that cropland expansion for BECCS causes a carbon loss even in low-carbon uptake lands and reduces the future potential increase in the global carbon uptake via LUC impact on the carbon stock, and the carbon-concentration and carbon-climate feedbacks. Under the SSP5-3.4-OS, the LUC emissions from BECCS deployment cause a decrease in global CO_2 fertilization effect-driven carbon uptake and increase the climate change-driven carbon loss.

Our results are consistent with the IPCC special report on climate change and land (Shukla et al., 2019) and highlight the need for considering trade-offs in BECCS deployment and other land-uses but, to some extent, they go beyond this assessment by considering the implication of carbon cycle feedbacks. Our work shows that areas best suited for BECCS should also be assessed both in terms of their potential amount of the bioenergy yield and potential future impact on the carbon-climate feedbacks. Future studies need to further investigate the potential of BECCS to provide negative carbon emissions with little loss of storage from the LUC.

Data availability

Author Contributions

374 **Competing Interests**

376 **Acknowledgments**

397

Appendix

Text A1. Sensitivity study for deriving the crop-concentrated grid thresholds

Neither IAMs nor ESMs provide BECCS-related LUC emissions. Separating BECCS-related emissions from all other LUC emissions is virtually impossible due to spatial heterogeneity and many complex factors that affect the bioenergy crop deployment.

ESMs do not distinguish second-generation bioenergy crops from other crops in CMIP6. Moreover, the cropland area in ESMs is defined at a sub-grid scale (i.e., on a fraction or tile of a grid box). Because land-use states (e.g., forest, crops, pastures) vary in productivity and, thus, carbon uptakes and because modelling teams do not provide NBP estimates at the sub-grid level, to estimate the area and carbon fluxes of the biofuel crops in ESMs, we assume that all croplands deployed after the 2040s are for second-generation biofuel crops (Figure A1). We label the given grid of CMIP6 simulation outputs as crop-concentrated if the cropland fraction of the grid is larger than a given threshold derived via a sensitivity analysis (Figure A1).
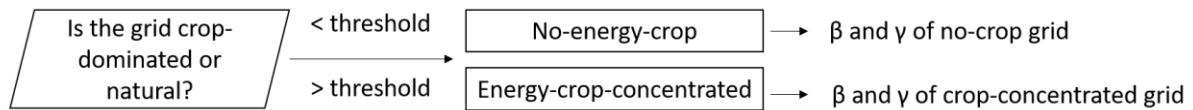

Figure A1: A schematic presentation of the sensitivity study for estimating the carbon-climate feedback parameters over the energy-crop-concentrated and no-energy-crop grids.

We examined time-invariant cropland fraction thresholds ranging from 25% to 45% of the grid box area and selected a range of thresholds that best approximate the change in the total cropland area of each ESM in 2015–2100 (Figure A2). Here we choose the fitting period of 2015–2100 because a shorter period (2040–2100) would result in a lower threshold during the 2050–2060 period with a large global cropland increase. More specifically, we selected a range of thresholds with a 1%-step so that they intersect at least once either the global cropland area estimated by ESM itself or LUH2 data set from 2015 to 2100. Although the selected ensembles of thresholds are time-invariant, the resultant cropland area increases. We find that for a later period (end of the 21st century), a higher threshold is required because both the spatial coverage (the number of grid boxes that have crops) and cropland concentration (a grid fraction of cropland) increases (Figure A2).

We confirmed the spatial distribution of the minimum and maximum selected thresholds of energy-crop-concentrated grids against sub-grid scale ESM and the LUH2 estimates of cropland area (Figure A3).

424
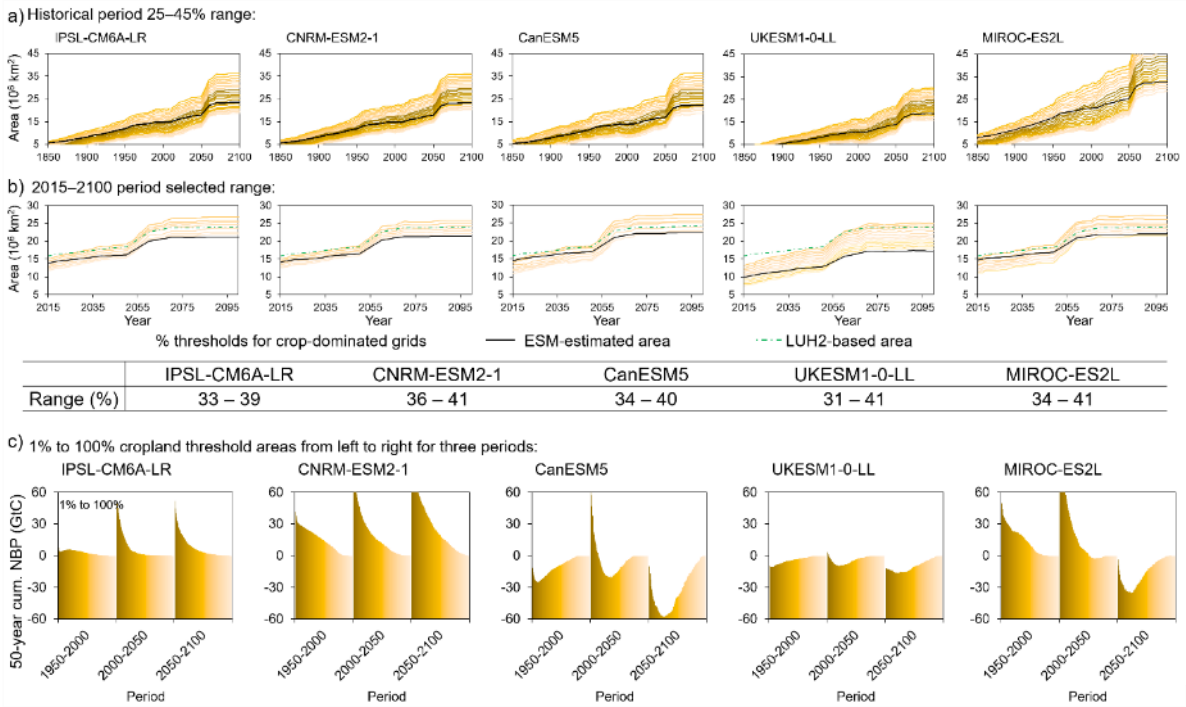
Figure A2: (a) The cropland-fraction thresholds ranging from 25% to 45% of the grid box area analyzed in the sensitivity study and (b) the selected (resultant) range of thresholds for identifying the energy-crop-concentrated area with the selected range for each ESM indicated in the table. Panel (c) shows the cumulative NBP of the areas corresponding to the range of cropland thresholds from 1 to 100% (left dark to right light color) in three periods.
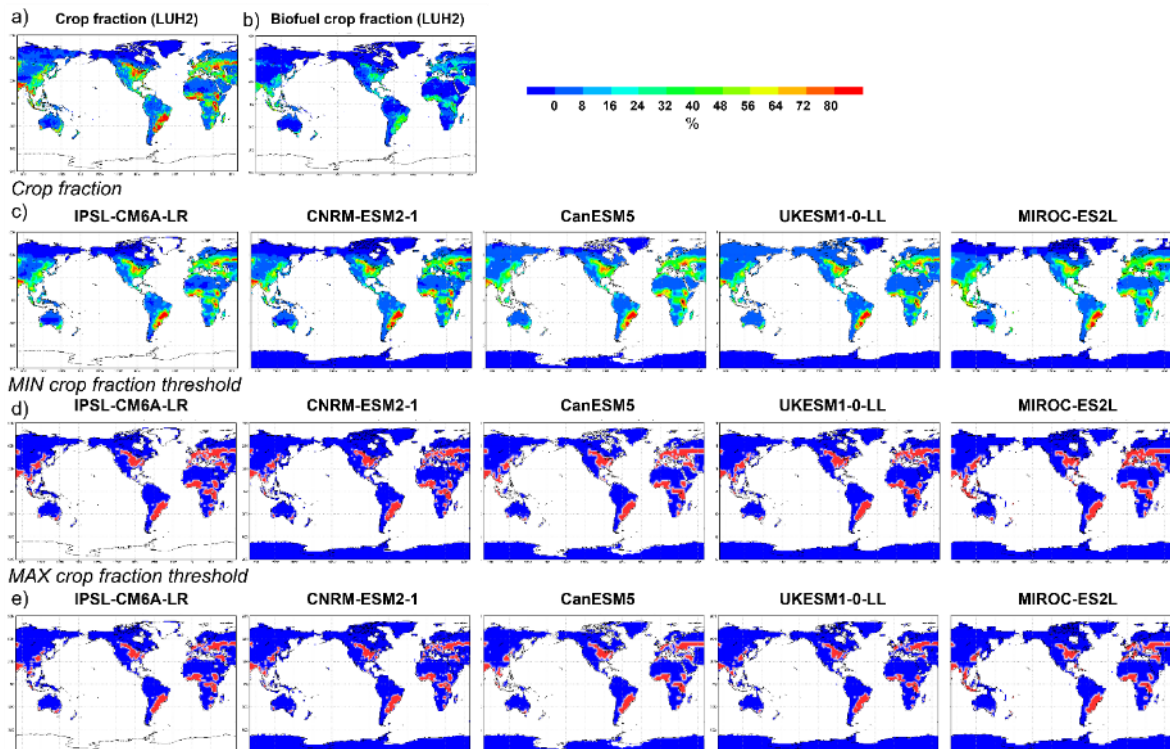
429
430 Figure A3: Spatial variation of (a) grid cropland fraction (b) and second-generation bioenergy cropland fraction by
431 LUH2. Panel (c) shows the spatial variation of grid cropland fraction estimated by CMIP6 ESMs. The spatial variation
432 of the selected (d) minimum and (e) maximum thresholds (that intersect at least once either the global cropland area
433 estimated by ESM itself or LUH2 data set from 2015 to 2100 as shown in Figure A1) for estimating crop-concentrated
434 grids in 2100.

435

13

436   **References**

437   Anderson, K. and Peters, G.: The trouble with negative emissions, Science, 354, 182,
438   https://doi.org/10.1126/science.aah4567, 2016.

439   Arora, V. K., Katavouta, A., Williams, R. G., Jones, C. D., Brovkin, V., Friedlingstein, P., Schwinger, J., Bopp,
440   L., Boucher, O., Cadule, P., Chamberlain, M. A., Christian, J. R., Delire, C., Fisher, R. A., Hajima, T., Ilyina, T.,
441   Joetzjer, E., Kawamiya, M., Koven, C. D., Krasting, J. P., Law, R. M., Lawrence, D. M., Lenton, A., Lindsay, K.,
442   Pongratz, J., Raddatz, T., Séférian, R., Tachiiri, K., Tjiputra, J. F., Wiltshire, A., Wu, T., and Ziehn, T.: Carbon–
443   concentration and carbon–climate feedbacks in CMIP6 models and their comparison to CMIP5 models,
444   Biogeosciences, 17, 4173–4222, https://doi.org/10.5194/bg-17-4173-2020, 2020.

445   Babin, A., Vaneeckhaute, C., and Iliuta, M. C.: Potential and challenges of bioenergy with carbon capture and
446   storage as a carbon-negative energy source: A review, Biomass and Bioenergy, 146, 105968,
447   https://doi.org/10.1016/j.biombioe.2021.105968, 2021.

448   Bauer, N., Calvin, K., Emmerling, J., Fricko, O., Fujimori, S., Hilaire, J., Eom, J., Krey, V., Kriegler, E.,
449   Mouratiadou, I., de Boer, H. S., van den Berg, M., Carrara, S., Daioglou, V., Drouet, L., Edmonds, J. E., Gernaat,
450   D., Havlik, P., Johnson, N., Klein, D., Kyle, P., Marangoni, G., Masui, T., Pietzcker, R. C., Strubegger, M., Wise,
451   M., Riahi, K., and van Vuuren, D. P.: Shared Socio-Economic Pathways of the Energy Sector – Quantifying the
452   Narratives, Glob. Environ. Change, 42, 316–330, https://doi.org/10.1016/j.gloenvcha.2016.07.006, 2017.

453   Boucher, O., Servonnat, J., Albright, A. L., Aumont, O., Balkanski, Y., Bastrikov, V., Bekki, S., Bonnet, R., Bony,
454   S., Bopp, L., Braconnot, P., Brockmann, P., Cadule, P., Caubel, A., Cheruy, F., Codron, F., Cozic, A., Cugnet,
455   D., D'Andrea, F., Davini, P., Lavergne, C. de, Denvil, S., Deshayes, J., Devilliers, M., Ducharne, A., Dufresne,
456   J.-L., Dupont, E., Éthé, C., Fairhead, L., Falletti, L., Flavoni, S., Foujols, M.-A., Gardoll, S., Gastineau, G.,
457   Ghattas, J., Grandpeix, J.-Y., Guenet, B., Guez, L., E., Guilyardi, E., Guimberteau, M., Hauglustaine, D., Hourdin,
458   F., Idelkadi, A., Joussaume, S., Kageyama, M., Khodri, M., Krinner, G., Lebas, N., Levavasseur, G., Lévy, C., Li,
459   L., Lott, F., Lurton, T., Luyssaert, S., Madec, G., Madeleine, J.-B., Maignan, F., Marchand, M., Marti, O., Mellul,
460   L., Meurdesoif, Y., Mignot, J., Musat, I., Ottlé, C., Peylin, P., Planton, Y., Polcher, J., Rio, C., Rochetin, N.,
461   Rousset, C., Sepulchre, P., Sima, A., Swingedouw, D., Thiéblemont, R., Traore, A. K., Vancoppenolle, M., Vial,
462   J., Vialard, J., Viovy, N., and Vuichard, N.: Presentation and Evaluation of the IPSL-CM6A-LR Climate Model,
463   J. Adv. Model Earth Sy., 12, e2019MS002010, https://doi.org/10.1029/2019MS002010, 2020.

464   Boysen, L. R., Brovkin, V., Wårlind, D., Peano, D., Lansø, A.S., Delire, C., Burke, E., Poeplau, C., and Don., A.:
465   Evaluation of soil carbon dynamics after forest cover change in CMIP6 land models using chronosequences.
466   Environ. Res. Lett, 16, 7, 074030, https://doi.org/10.1088/1748-9326/ac0be1, 2021

467   Campbell, J. E., Lobell, D. B., Genova, R. C., and Field, C. B.: The global potential of bioenergy on abandoned
468   agriculture lands, Environ Sci Technol., 42, 5791–5794, https://doi.org/10.1021/es800052w, 2008.

469   Canadell, J. G. and Schulze, E. D.: Global potential of biospheric carbon management for climate mitigation, Nat.
470   Commun., 5, 1–12, https://doi.org/10.1038/ncomms6282, 2014.

471   Clair, S. S., Hillier, J., and Smith, P.: Estimating the pre-harvest greenhouse gas costs of energy crop production,
472   Biomass Bioenerg., 32, 442–452, https://doi.org/10.1016/j.biombioe.2007.11.001, 2008.

473   Dooley, K., Christoff, P., and Nicholas, K. A.: Co-producing climate policy and negative emissions: trade-offs
474   for sustainable land-use, Global Sustainability, 1, https://doi.org/10.1017/sus.2018.6, 2018.

475   Erb, K.-H., Fetzel, T., Plutzar, C., Kastner, T., Lauk, C., Mayer, A., Niedertscheider, M., Körner, C., and Haberl,
476   H.: Biomass turnover time in terrestrial ecosystems halved by land use, Nature Geoscience, 9, 674–678,
477   https://doi.org/10.1038/ngeo2782, 2016.

478   Fargione, J., Hill, J., Tilman, D., Polasky, S., and Hawthorne, P.: Land Clearing and the Biofuel Carbon Debt,
479   Science, 319, 1235, https://doi.org/10.1126/science.1152747, 2008.

480   Friedlingstein, P., Cox, P., Betts, R., Bopp, L., von Bloh, W., Brovkin, V., Cadule, P., Doney, S., Eby, M., Fung,
481   I, Bala, G., John, J., Jones, C., Joos, F., Kato, T., Kawamiya, M., Knorr, W., Lindsay, K., Matthews, H. D.,
482   Raddatz, T., Rayner, P., Reick, C., Roeckner, E., Schnitzler, K.-G., Schnur, R., Strassmann, K., Weaver, A. J.,

14

Yoshikawa, C., and Zeng, N.: Climate–Carbon Cycle Feedback Analysis: Results from the C4MIP Model Intercomparison, J. Climate, 19, 3337–3353, https://doi.org/10.1175/JCLI3800.1, 2006.

Friedlingstein, P., O'Sullivan, M., Jones, M. W., Andrew, R. M., Hauck, J., Olsen, A., Peters, G. P., Peters, W., Pongratz, J., Sitch, S., Le Quéré, C., Canadell, J. G., Ciais, P., Jackson, R. B., Alin, S., Aragão, L. E. O. C., Arneth, A., Arora, V., Bates, N. R., Becker, M., Benoit-Cattin, A., Bittig, H. C., Bopp, L., Bultan, S., Chandra, N., Chevallier, F., Chini, L. P., Evans, W., Florentie, L., Forster, P. M., Gasser, T., Gehlen, M., Gilfillan, D., Gkritzalis, T., Gregor, L., Gruber, N., Harris, I., Hartung, K., Haverd, V., Houghton, R. A., Ilyina, T., Jain, A. K., Joetzjer, E., Kadono, K., Kato, E., Kitidis, V., Korsbakken, J. I., Landschützer, P., Lefèvre, N., Lenton, A., Lienert, S., Liu, Z., Lombardozzi, D., Marland, G., Metzl, N., Munro, D. R., Nabel, J. E. M. S., Nakaoka, S.-I., Niwa, Y., O'Brien, K., Ono, T., Palmer, P. I., Pierrot, D., Poulter, B., Resplandy, L., Robertson, E., Rödenbeck, C., Schwinger, J., Séférian, R., Skjelvan, I., Smith, A. J. P., Sutton, A. J., Tanhua, T., Tans, P. P., Tian, H., Tilbrook, B., van der Werf, G., Vuichard, N., Walker, A. P., Wanninkhof, R., Watson, A. J., Willis, D., Wiltshire, A. J., Yuan, W., Yue, X., and Zaehle, S.: Global Carbon Budget 2020, Earth Syst. Sci. Data, 12, 3269–3340, https://doi.org/10.5194/essd-12-3269-2020, 2020.

Gasser, T. and Ciais, P.: A theoretical framework for the net land-to-atmosphere CO_2 flux and its implications in the definition of "emissions from land-use change", Earth Syst. Dynam., 4, 171–186, https://doi.org/10.5194/esd-4-171-2013, 2013.

Gasser, T., Crepin, L., Quilcaille, Y., Houghton, R. A., Ciais, P., and Obersteiner, M.: Historical CO_2 emissions from land use and land cover change and their uncertainty, Biogeosciences, 17, 4075–4101, https://doi.org/10.5194/bg-17-4075-2020, 2020.

Gibbs, H. K., Johnston, M., Foley, J. A., Holloway, T., Monfreda, C., Ramankutty, N., and Zaks, D.: Carbon payback times for crop-based biofuel expansion in the tropics: the effects of changing yield and technology, Environ Res Lett., 3, 034001, https://doi.org/10.1088/1748-9326/3/3/034001, 2008.

Gregory, J. M., Jones, C. D., Cadule, P., and Friedlingstein, P.: Quantifying Carbon Cycle Feedbacks, J. Climate, 22, 5232–5250, https://doi.org/10.1175/2009JCLI2949.1, 2009.

Hajima, T., Watanabe, M., Yamamoto, A., Tatebe, H., Noguchi, M. A., Abe, M., Ohgaito, R., Ito, A., Yamazaki, D., Okajima, H., Ito, A., Takata, K., Ogochi, K., Watanabe, S., and Kawamiya, M.: Development of the MIROC-ES2L Earth system model and the evaluation of biogeochemical processes and feedbacks, Geosci. Model Dev., 13, 2197–2244, https://doi.org/10.5194/gmd-13-2197-2020, 2020.

Hansis, E., Davis, S. J., and Pongratz, J.: Relevance of methodological choices for accounting of land use change carbon fluxes, Global. Biogeochem. Cy., 29, 1230–1246, https://doi.org/10.1002/2014GB004997, 2015.

Harper, A. B., Powell, T., Cox, P. M., House, J., Huntingford, C., Lenton, T. M., Sitch, S., Burke, E., Chadburn, S. E., Collins, W. J., Comyn-Platt, E., Daioglou, V., Doelman, J. C., Hayman, G., Robertson, E., van Vuuren, D., Wiltshire, A., Webber, C. P., Bastos, A., Boysen, L., Ciais, P., Devaraju, N., Jain, A. K., Krause, A., Poulter, B., and Shu, S.: Land-use emissions play a critical role in land-based mitigation for Paris climate targets, Nat. Commun., 9, 2938, https://doi.org/10.1038/s41467-018-05340-z, 2018.

Heck, V., Gerten, D., Lucht, W., and Popp, A.: Biomass-based negative emissions difficult to reconcile with planetary boundaries, Nat. Clim. Change, 8, 151–155, https://doi.org/10.1038/s41558-017-0064-y, 2018.

Houghton, R. A. and Nassikas, A. A.: Global and regional fluxes of carbon from land use and land cover change 1850–2015, Global. Biogeochem. Cy., 31, 456–472, https://doi.org/10.1002/2016GB005546, 2017.

Hurtt, G. C., Chini, L., Sahajpal, R., Frolking, S., Bodirsky, B. L., Calvin, K., Doelman, J. C., Fisk, J., Fujimori, S., Goldewijk, K. K., Hasegawa, T., Havlik, P., Heinimann, A., Humpenöder, F., Jungclaus, J., Kaplan, J., Kennedy, J., Kristzin, T., Lawrence, D., Lawrence, P., Ma, L., Mertz, O., Pongratz, J., Popp, A., Poulter, B., Riahi, K., Shevliakova, E., Stehfest, E., Thornton, P., Tubiello, F. N., van Vuuren, D. P., and Zhang, X.: Harmonization of Global Land-Use Change and Management for the Period 850-2100 (LUH2) for CMIP6, Geosci Model Dev., 1–65, https://doi.org/10.5194/gmd-2019-360, 2020.

Jones, C. D., Arora, V., Friedlingstein, P., Bopp, L., Brovkin, V., Dunne, J., Graven, H., Hoffman, F., Ilyina, T., John, J. G., Jung, M., Kawamiya, M., Koven, C., Pongratz, J., Raddatz, T., Randerson, J. T., and Zaehle, S.:

531   C4MIP - The Coupled Climate–Carbon Cycle Model Intercomparison Project: experimental protocol for CMIP6,
532   Geosci. Model Dev., 9, 2853–2880, https://doi.org/10.5194/gmd-9-2853-2016, 2016a.

533   Jones, C. D., Ciais, P., Davis, S. J., Friedlingstein, P., Gasser, T., Peters, G. P., Rogelj, J., van Vuuren, D. P.,
534   Canadell, J. G., Cowie, A., Jackson, R. B., Jonas, M., Kriegler, E., Littleton, E., Lowe, J. A., Milne, J., Shrestha,
535   G., Smith, P., Torvanger, A., and Wiltshire, A.: Simulating the Earth system response to negative emissions,
536   Environ. Res. Lett., 11, 095012, https://doi.org/10.1088/1748-9326/11/9/095012, 2016b.

537   Jones, M. B. and Albanito, F.: Can biomass supply meet the demands of bioenergy with carbon capture and storage
538   (BECCS)?, Glob. Change Biol., 26, 5358–5364, https://doi.org/10.1111/gcb.15296, 2020.

539   Keller, D. P., Lenton, A., Scott, V., Vaughan, N. E., Bauer, N., Ji, D., Jones, C. D., Kravitz, B., Muri, H., and
540   Zickfeld, K.: The Carbon Dioxide Removal Model Intercomparison Project (CDRMIP): rationale and
541   experimental protocol for CMIP6, Geosci. Model Dev., 11, 1133–1160, https://doi.org/10.5194/gmd-11-1133-
542   2018, 2018.

543   Krause, A., Pugh, T. A. M., Bayer, A. D., Li, W., Leung, F., Bondeau, A., Doelman, J. C., Humpenöder, F.,
544   Anthoni, P., Bodirsky, B. L., Ciais, P., Müller, C., Murray-Tortarolo, G., Olin, S., Popp, A., Sitch, S., Stehfest,
545   E., and Arneth, A.: Large uncertainty in carbon uptake potential of land-based climate-change mitigation efforts,
546   Glob. Change Biol., 24, 3025–3038, https://doi.org/10.1111/gcb.14144, 2018.

547   Kriegler, E., Bauer, N., Popp, A., Humpenöder, F., Leimbach, M., Strefler, J., Baumstark, L., Bodirsky, B. L.,
548   Hilaire, J., Klein, D., Mouratiadou, I., Weindl, I., Bertram, C., Dietrich, J.-P., Luderer, G., Pehl, M., Pietzcker, R.,
549   Piontek, F., Lotze-Campen, H., Biewald, A., Bonsch, M., Giannousakis, A., Kreidenweis, U., Müller, C., Rolinski,
550   S., Schultes, A., Schwanitz, J., Stevanovic, M., Calvin, K., Emmerling, J., Fujimori, S., and Edenhofer, O.: Fossil-
551   fueled development (SSP5): An energy and resource intensive scenario for the 21st century, Glob. Environ.
552   Change, 42, 297–315, https://doi.org/10.1016/j.gloenvcha.2016.05.015, 2017.

553   Li, W., Ciais, P., Han, M., Zhao, Q., Chang, J., Goll, D. S., Zhu, L., and Wang, J.: Bioenergy Crops for Low
554   Warming Targets Require Half of the Present Agricultural Fertilizer Use, Environ. Sci. Technol., 55, 10654–
555   10661, https://doi.org/10.1021/acs.est.1c02238, 2021.

556   Liddicoat, S. K., Wiltshire, A. J., Jones, C. D., Arora, V. K., Brovkin, V., Cadule, P., Hajima, T., Lawrence, D.
557   M., Pongratz, J., and Schwinger, J.: Compatible Fossil Fuel CO2 Emissions in the CMIP6 Earth System Models'
558   Historical and Shared Socioeconomic Pathway Experiments of the Twenty-First Century, J. Climate, 34, 2853–
559   2875, https://doi.org/10.1175/JCLI-D-19-0991.1, 2021.

560   Meinshausen, M., Nicholls, Z. R. J., Lewis, J., Gidden, M. J., Vogel, E., Freund, M., Beyerle, U., Gessner, C.,
561   Nauels, A., Bauer, N., Canadell, J. G., Daniel, J. S., John, A., Krummel, P. B., Luderer, G., Meinshausen, N.,
562   Montzka, S. A., Rayner, P. J., Reimann, S., Smith, S. J., van den Berg, M., Velders, G. J. M., Vollmer, M. K., and
563   Wang, R. H. J.: The shared socio-economic pathway (SSP) greenhouse gas concentrations and their extensions to
564   2500, Geosci. Model Dev., 13, 3571–3605, https://doi.org/10.5194/gmd-13-3571-2020, 2020.

565   Melnikova, I., Boucher, O., Cadule, P., Ciais, P., Gasser, T., Quilcaille, Y., Shiogama, H., Tachiiri, K., Yokohata,
566   T., and Tanaka, K.: Carbon cycle response to temperature overshoot beyond 2 °C – an analysis of CMIP6 models,
567   Earth's Future, 9, e2020EF001967, https://doi.org/10.1029/2020EF001967, 2021.

568   Mohr, A. and Raman, S.: Lessons from first generation biofuels and implications for the sustainability appraisal
569   of second generation biofuels, Energy Policy, 63, 114–122, https://doi.org/10.1016/j.enpol.2013.08.033, 2013.

570   O'Neill, B. C., Tebaldi, C., Van Vuuren, D. P., Eyring, V., Friedlingstein, P., Hurtt, G., Knutti, R., Kriegler, E.,
571   Lamarque, J. F., Lowe, J., Meehl, G. A., Moss, R., Riahi, K., and Sanderson, B. M.: The Scenario Model
572   Intercomparison Project (ScenarioMIP) for CMIP6, Geosci. Model Dev., 9, https://doi.org/10.5194/gmd-9-3461-
573   2016, 2016.

574   Pongratz, J., Reick, C. H., Houghton, R. A., and House, J. I.: Terminology as a key uncertainty in net land use
575   and land cover change carbon flux estimates, Earth Syst. Dynam., 5, 177–195, https://doi.org/10.5194/esd-5-177-
576   2014, 2014.

577 Popp, A., Calvin, K., Fujimori, S., Havlik, P., Humpenöder, F., Stehfest, E., Bodirsky, B. L., Dietrich, J. P.,
578 Doelmann, J. C., Gusti, M., Hasegawa, T., Kyle, P., Obersteiner, M., Tabeau, A., Takahashi, K., Valin, H.,
579 Waldhoff, S., Weindl, I., Wise, M., Kriegler, E., Lotze-Campen, H., Fricko, O., Riahi, K., and van Vuuren, D. P.:
580 Land-use futures in the shared socio-economic pathways, Glob. Environ. Change, 42, 331–345,
581 https://doi.org/10.1016/j.gloenvcha.2016.10.002, 2017.

582 Riahi, K., van Vuuren, D. P., Kriegler, E., Edmonds, J., O'Neill, B. C., Fujimori, S., Bauer, N., Calvin, K., Dellink,
583 R., Fricko, O., Lutz, W., Popp, A., Cuaresma, J. C., Samir, K. C., Leimbach, M., Jiang, L., Kram, T., Rao, S.,
584 Emmerling, J., Ebi, K., Hasegawa, T., Havlik, P., Humpenöder, F., Silva, L. A. D., Smith, S., Stehfest, E., Bosetti,
585 V., Eom, J., Gernaat, D., Masui, T., Rogelj, J., Strefler, J., Drouet, L., Krey, V., Luderer, G., Harmsen, M.,
586 Takahashi, K., Baumstark, L., Doelman, J. C., Kainuma, M., Klimont, Z., Marangoni, G., Lotze-Campen, H.,
587 Obersteiner, M., Tabeau, A., and Tavoni, M.: The Shared Socioeconomic Pathways and their energy, land use,
588 and greenhouse gas emissions implications: An overview, Glob. Environ. Change, 42, 153–168,
589 https://doi.org/10.1016/j.gloenvcha.2016.05.009, 2017.

590 Rogelj, J., Shindell, D., Jiang, K., Fifita, S., Forster, P., Ginzburg, V., Handa, C., Kheshgi, H., Kobayashi, S.,
591 Kriegler, E., Mundaca, L., Séférian, R., Vilarino, M. V., Calvin, K., de Oliveira de Portugal Pereira, J. C.,
592 Edelenbosch, O., Emmerling, J., Fuss, S., Gasser, T., Gillett, N., He, C., Hertwich, E., Höglund-Isaksson, L.,
593 Huppmann, D., Luderer, G., Markandya, A., Meinshausen, M., McCollum, D., Millar, R., Popp, A., Purohit, P.,
594 Riahi, K., Ribes, A., Saunders, H., Schädel, C., Smith, C., Smith, P., Trutnevyte, E., Xu, Y., Zhou, W., Zickfeld,
595 K., Mitigation Pathways Compatible with 1.5°C in the Context of Sustainable Development. - In: Masson-
596 Delmotte, V., Zhai, P., Pörtner, H. O., Roberts, D., Skea, J., Shukla, P. R., Pirani, A., Moufouma-Okia, W., Péan,
597 C., Pidcock, R., Connors, S., Matthews, J. B. R., Chen, Y., Zhou, X., Zhou, M. I., Lonnoy, E., Maycock, T.,
598 Tignor, M., Waterfield, T. (Eds.), Global warming of 1.5 °C, (IPCC Special Report), Geneva: Intergovernmental
599 Panel on Climate Change, 93-174, 2018.

600 Schueler, V., Weddige, U., Beringer, T., Gamba, L., and Lamers, P.: Global biomass potentials under
601 sustainability restrictions defined by the European Renewable Energy Directive 2009/28/EC, GCB Bioenergy, 5,
602 652–663, https://doi.org/10.1111/gcbb.12036, 2013.

603 Schwinger, J. and Tjiputra, J.: Ocean Carbon Cycle Feedbacks Under Negative Emissions, Geophys. Res. Lett.,
604 45, 5062–5070, https://doi.org/10.1029/2018GL077790, 2018.

605 Séférian, R., Rocher, M., Guivarch, C., and Colin, J.: Constraints on biomass energy deployment in mitigation
606 pathways: the case of water scarcity, Environ. Res. Lett., 13, 054011, https://doi.org/10.1088/1748-9326/aabcd7,
607 2018.

608 Séférian, R., Nabat, P., Michou, M., Saint-Martin, D., Voldoire, A., Colin, J., Decharme, B., Delire, C., Berthet,
609 S., Chevallier, M., Sénési, S., Franchisteguy, L., Vial, J., Mallet, M., Joetzjer, E., Geoffroy, O., Guérémy, J.-F.,
610 Moine, M.-P., Msadek, R., Ribes, A., Rocher, M., Roehrig, R., Salas-y-Mélia, D., Sanchez, E., Terray, L., Valcke,
611 S., Waldman, R., Aumont, O., Bopp, L., Deshayes, J., Éthé, C., and Madec, G.: Evaluation of CNRM Earth
612 System Model, CNRM-ESM2-1: Role of Earth System Processes in Present-Day and Future Climate, J. Adv.
613 Model Earth Sy., 11, 4182–4227, https://doi.org/10.1029/2019MS001791, 2019.

614 Sellar, A. A., Jones, C. G., Mulcahy, J. P., Tang, Y., Yool, A., Wiltshire, A., O'Connor, F. M., Stringer, M., Hill,
615 R., Palmieri, J., Woodward, S., Mora, L. de, Kuhlbrodt, T., Rumbold, S. T., Kelley, D. I., Ellis, R., Johnson, C.
616 E., Walton, J., Abraham, N. L., Andrews, M. B., Andrews, T., Archibald, A. T., Berthou, S., Burke, E., Blockley,
617 E., Carslaw, K., Dalvi, M., Edwards, J., Folberth, G. A., Gedney, N., Griffiths, P. T., Harper, A. B., Hendry, M.
618 A., Hewitt, A. J., Johnson, B., Jones, A., Jones, C. D., Keeble, J., Liddicoat, S., Morgenstern, O., Parker, R. J.,
619 Predoi, V., Robertson, E., Siahaan, A., Smith, R. S., Swaminathan, R., Woodhouse, M. T., Zeng, G., and
620 Zerroukat, M.: UKESM1: Description and Evaluation of the U.K. Earth System Model, J. Adv. Model Earth Sy.,
621 11, 4513–4558, https://doi.org/10.1029/2019MS001739, 2019.

622 Shukla, P. R., Skea, J., Calvo Buendia, E., Masson-Delmotte, V., Pörtner, H. O., Roberts, D. C., Zhai, P., Slade,
623 R., Connors, S., and Van Diemen, R.: IPCC, 2019: Climate Change and Land: an IPCC special report on climate
624 change, desertification, land degradation, sustainable land management, food security, and greenhouse gas fluxes
625 in terrestrial ecosystems, 2019.

626 Smith, P., Davis, S. J., Creutzig, F., Fuss, S., Minx, J., Gabrielle, B., Kato, E., Jackson, R. B., Cowie, A., and
627 Kriegler, E.: Biophysical and economic limits to negative CO2 emissions, Nat. Clim. Change, 6, 42–50,
628 https://doi.org/10.1038/nclimate2870, 2016.

629 Swart, N. C., Cole, J. N. S., Kharin, V. V., Lazare, M., Scinocca, J. F., Gillett, N. P., Anstey, J., Arora, V.,
630 Christian, J. R., Hanna, S., Jiao, Y., Lee, W. G., Majaess, F., Saenko, O. A., Seiler, C., Seinen, C., Shao, A.,
631 Sigmond, M., Solheim, L., von Salzen, K., Yang, D., and Winter, B.: The Canadian Earth System Model version
632 5 (CanESM5.0.3), Geosci. Model Dev., 12, 4823–4873, https://doi.org/10.5194/gmd-12-4823-2019, 2019.

633 Tanaka, K., Boucher, O., Ciais, P., Johansson, D. J. A., and Morfeldt, J.: Cost-effective implementation of the
634 Paris Agreement using flexible greenhouse gas metrics, Sci Adv, 7, eabf9020,
635 https://doi.org/10.1126/sciadv.abf9020, 2021.

636 Whitaker, J., Field, J. L., Bernacchi, C. J., Cerri, C. E. P., Ceulemans, R., Davies, C. A., DeLucia, E. H., Donnison,
637 I. S., McCalmont, J. P., Paustian, K., Rowe, R. L., Smith, P., Thornley, P., and McNamara, N. P.: Consensus,
638 uncertainties and challenges for perennial bioenergy crops and land use, GCB Bioenergy, 10, 150–164,
639 https://doi.org/10.1111/gcbb.12488, 2018.

640 Wu, D., Piao, S., Zhu, D., Wang, X., Ciais, P., Bastos, A., Xu, X., and Xu, W.: Accelerated terrestrial ecosystem
641 carbon turnover and its drivers, Globa. Change Biol., 26, 5052–5062, https://doi.org/10.1111/gcb.15224, 2020.

642 Zhang, X., Wang, Y.P., Rayner, P.J., Ciais, P., Huang, K., Luo, Y., Piao, S., Wang, Z., Xia, J., Zhao, W. and
643 Zheng, X.. A small climate-amplifying effect of climate-carbon cycle feedback, Nature communications, 12(1):
644 1-11, https://doi.org/10.1038/s41467-021-22392-w, 2021.

Tables & figures

646

647 **Table 1. Major characteristics of the Earth system models.**

ESM*	Reference	Land carbon model and resolution	Inclusion of "fLuc"	Processes included to "fLuc"	Treatment of LUH2 pastures and rangelands
IPSL-CM6A-LR	(Boucher et al., 2020)	ORCHIDEE, br.2.0 144 × 143	Yes	deforestation	Pastures correspond to grass PFTs, rangelands – natural PFTs
CNRM-ESM2-1	(Séférian et al., 2019)	ISBA-CTRIP 256 × 128	Yes	deforestation decomposition	Pastures correspond to grasslands, rangelands – to shrubs
CanESM5	(Swart et al., 2019)	CLASS-CTEM 128 × 64	No		Not treated. Can be grasslands or shrubs
UKESM1-0-LL	(Sellar et al., 2019)	JULES-ES-1.0 192 × 144	Yes (excluded)	deforestation wood harvest decomposition	Pastures are managed grasslands; rangelands correspond to natural PFTs
MIROC-ES2L	(Hajima et al., 2020)	VISIT-e 128 × 64	No		The "closed pasture" and "rangeland" – natural vegetation, can be grasses or shrubs that get impact from grazing pressure

648 *DOIs of simulations by each ESM are provided in Table S1.
649
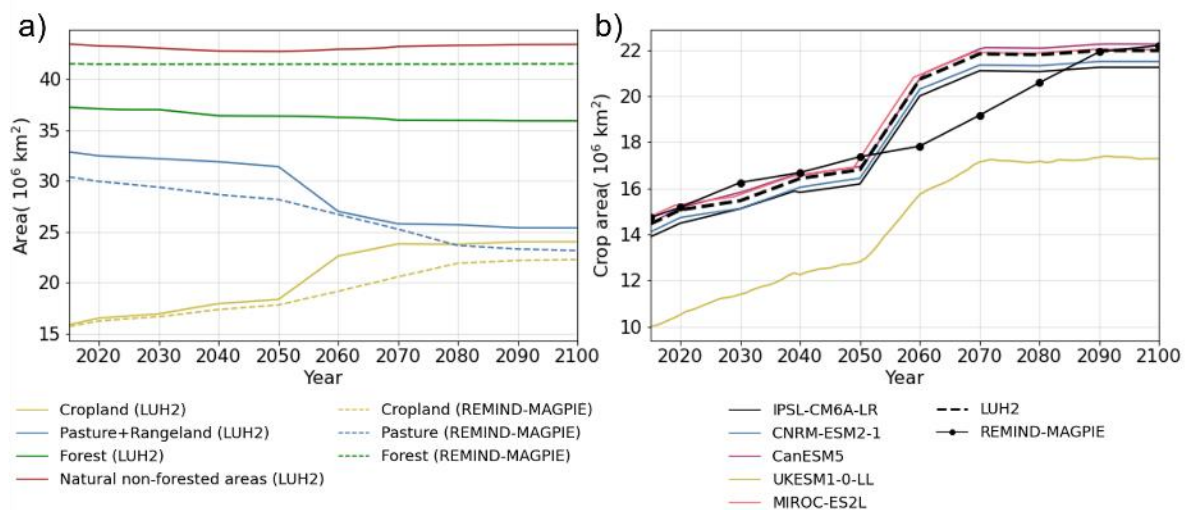
650
651 **Figure 1: Time series of (a) the changes in the area of croplands, pastures, and forests according to REMIND-MAgPIE**
652 **and LUH2, and (b) the area of croplands in LUH2, REMIND-MAgPIE, and five CMIP6 ESMs under the SSP5-3.4-OS**
653 **pathway. In panel (a), pastures and rangelands of LUH2 are treated together as pastures.**
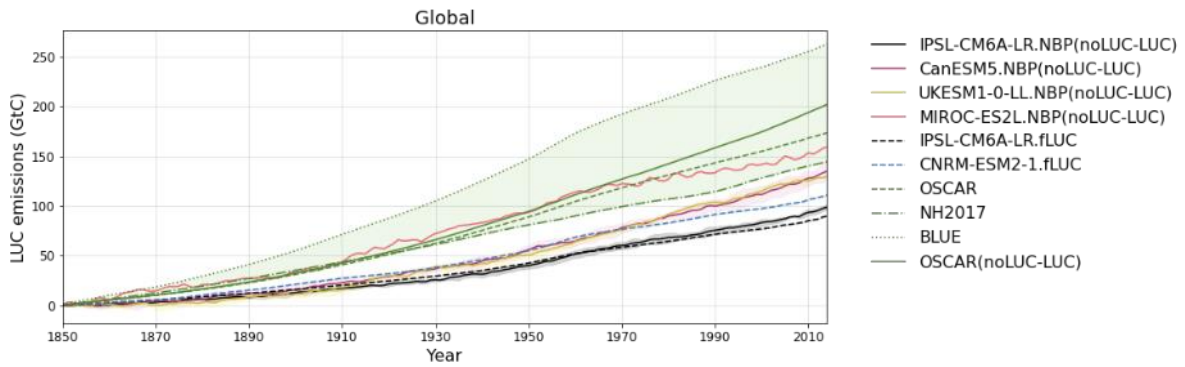
Figure 2: Evaluation of cumulative global LUC emissions by ESMs against three bookkeeping models. LUC emissions are defined by two methods: 1) the difference in NBP between simulations with and without LUC (solid lines) and 2) the "fLuc" variable provided in CMIP6 (dashed lines). The estimates of the bookkeeping approach using OSCAR are shown for cases with (noLUC-LUC) and without LASC). The range of bookkeeping models is shaded green.
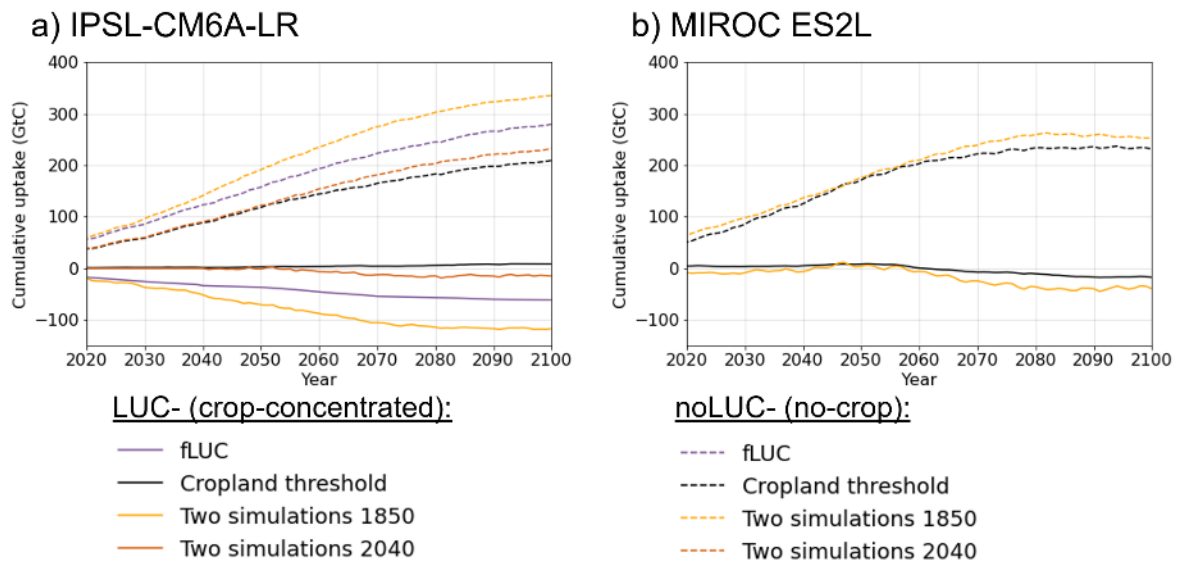

Figure 3: Cumulative land carbon uptake from the year 2000 in LUC-concentrated (solid lines) and noLUC (dashed lines) ecosystems estimated by three approaches by (a) IPSL-CM6A-LR and (b) MIROC-ES2L.
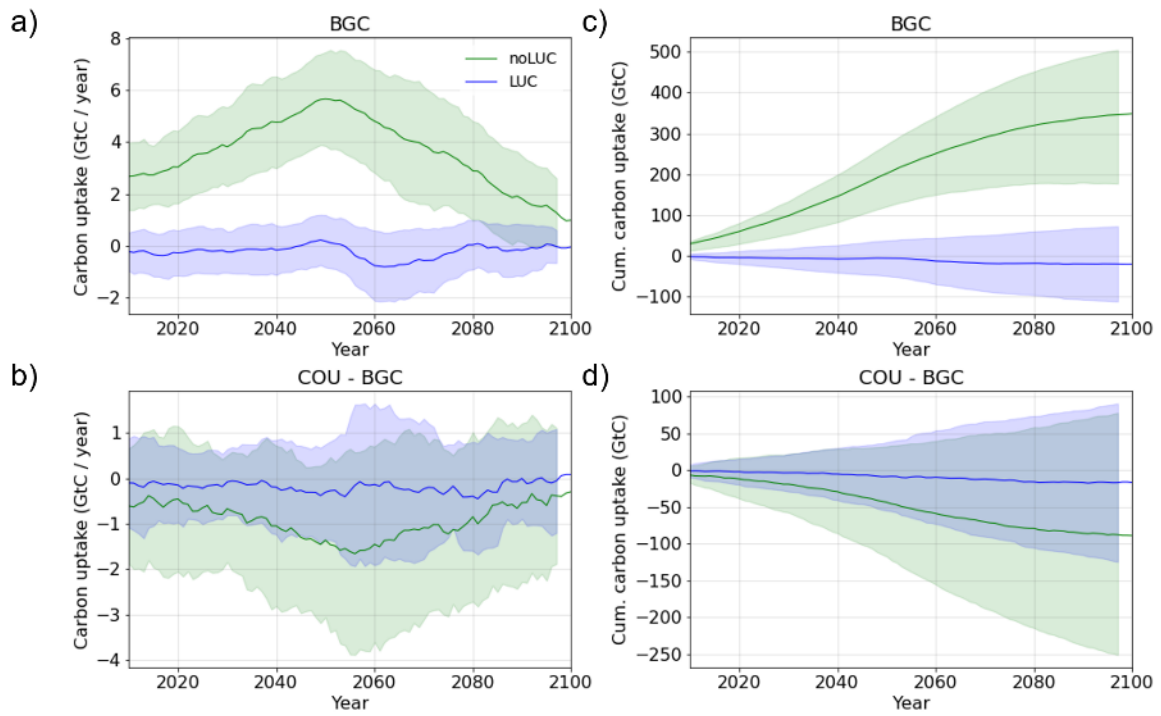
665
666 Figure 4: Interannual variation of global (a, b) land carbon uptake and (c, d) cumulative carbon uptake in LUC-
667 concentrated and noLUC ecosystems given as mean and standard deviation (shaded area) of five ESMs and three
668 approaches. Panels a and c show BGC simulation outputs, and panels b and d show the difference in COU and BGC
669 simulation outputs.

a) IPSL-CM6A-LR

b) MIROC-ES2L

LUC

noLUC

c) Bioenergy crop fraction in 2100 from LUH2

670
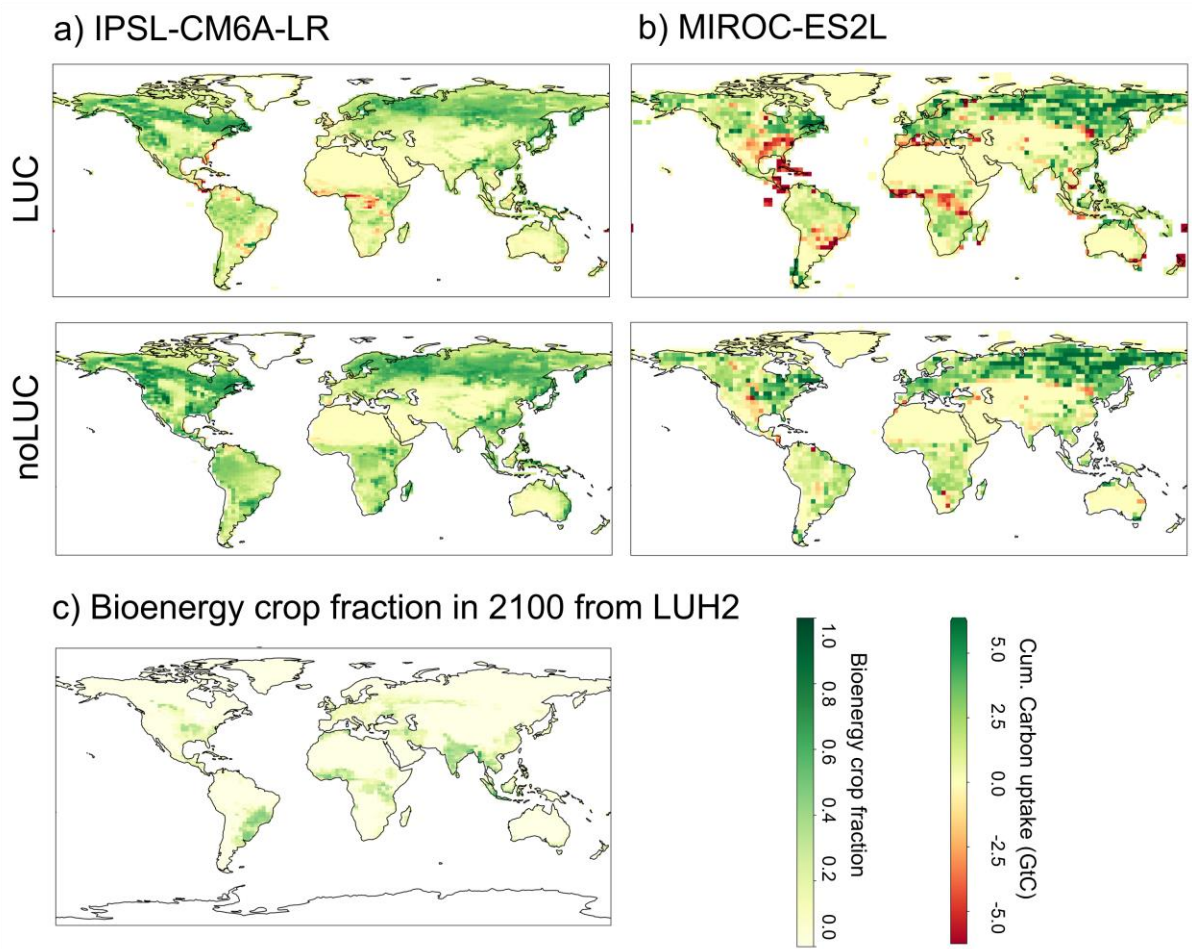
Figure 5: Spatial variations of the cumulative over 2040 – 2100 period carbon uptake by (a) IPSL-CM6A-LR and (b) MIROC-ES2L given for the fully coupled simulations with and without LUC. The negative values indicate less sink / larger source from land to atmosphere. (c) The bioenergy crop area in 2100 from LUH2.

22

674
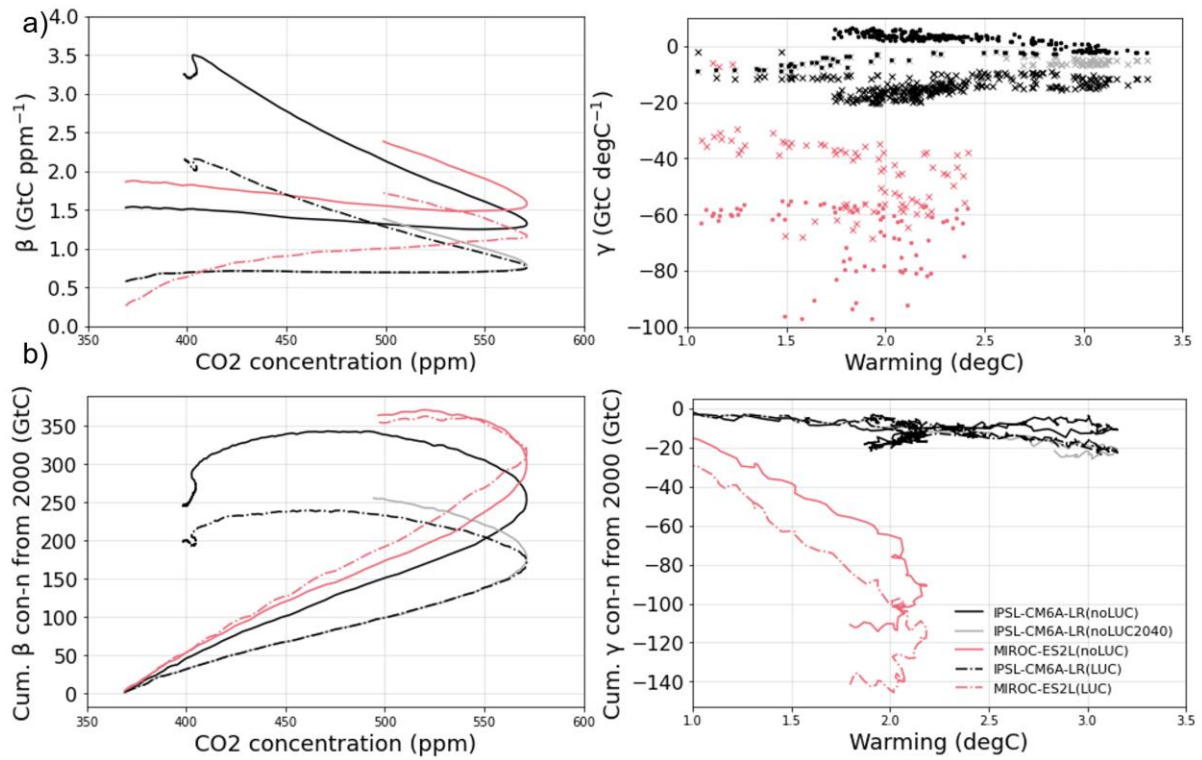
Figure 6: The variation of (a) global β_{land} (GtC ppm^{-1}) and γ_{land} (GtC °C^{-1}), and (b) cumulative over 2000–2300 (for IPSL-CM6A-LR) and over 2000–2100 (for MIROC-ES2L) β- and γ-driven land carbon uptakes with and without LUC. The changes in LUC are given as 9-year moving averages, negative value corresponds to a land sink.